A Novel Crown Ether Generation Containing Different Heteroaromatic Cations: Synthesis, Characterization, Solid-Phase ^{13}C NMR, X-ray Crystal Structure, and Selective Amino Acid Recognition

Abolghasem Moghimi*

Department of Chemistry, University of Imam Hossein, Tehran, Iran

Majid Faal Rastegar, Mehdi Ghandi, and Masoud Taghizadeh

Department of Chemistry, University of Tehran, Tehran, Iran

Abdollah Yari and Mojtaba Shamsipur

Department of Chemistry, University of Razi, Kermanshah, Iran

Glenn P. A. Yap

Ottawa-Carleton Chemistry Institute, Department of Chemistry, University of Ottawa, Ottawa, Canada K1A 6N5

Hamid Rahbarnoohi

Department of Chemistry, Wayne State University, Detroit, Michigan

samoghimi@yahoo.com.

Received August 24, 2001

The synthesis and structural characterization of a novel generation of crown ethers, **3**, **5** and **6** containing pyrilium, thiopyrilium, and pyridinium subunits, respectively, are reported. The crown ether unit is potentially capable of forming host−guest complexes with inorganic and organic cations, while the heteroaromatic cationic unit is suitable to bind with anions. A variety of physicochemical methods including electrospray mass spectrometry, UV−vis spectroscopy, solution and solid-phase NMR, and X-ray crystallography were applied for structural characterization of the new crown ether derivatives. The ^{1}H and ^{13}C NMR studies indicate rapid rotation of the B9C3 unit about the C−C bond that connects the two units to each other. Single crystals for **3**, **4**, and **5** were successfully obtained, and their X-ray crystal structures were resolved. The perchlorate anion in **3** (orthorhombic, space group $P2_12_12_1$) and **5** (orthorhombic, space group $P2_1$) is far from O^+ and close to S^+. The solid-phase structure of **3** and **5** show small deviation from planarity for the four aromatic rings, whereas two of the aromatic rings in **4** are out of heteroaromatic ring. Spectrophotometric studies in methanol solution revealed that the ligand **3** can be successfully applied to selective amino acid recognition.

Introduction

An extensive effort has already been made on the synthesis and structural properties of crown ethers[1−5] and heteroaromatic cations [6−10] as two important organic class of compounds. Because of their specific metal ion complexing ability and high extraction efficiency, crown ethers have been widely used as suitable neutral carriers in such important applications as selective metal transport through liquid membranes,[11] preparation of ion-selective membrane sensors,[12] and phase transfer catalysis.[13] Meanwhile, heteroaromatic cations have found valuable applications,[9,14,15] as indicated by an increasing number of patents,[15] as laser dyes, photosensitizers, and organic conductors.

(1) (a) Pedersen, C. J. *J. Am. Chem. Soc.* **1967**, *89*, 2495. (b) Pedersen, C. J. *J. Am. Chem. Soc.* **1967**, *89*, 7017. (c) Pedersen, C. J. *J. Org. Chem.* **1971**, *36*, 1690.

(2) (a) Izatt, R. M.; Pawlak, K.; Bradshow, J. S.; Bruening, R. L. *Chem. Rev.* **1995**, *95*, 2529. (b) Vogtle, F.; Muller, M. W.; Watson, W. H. *Top. Curr. Chem.* **1984**, *125*, 131. (c) Kimura, K.; Yamashita, T.; Kaneshige, M. Yokoyama, M. *J. Chem. Soc., Chem. Commun.* **1992**, 969. (d) Lee, W. Y.; Park, C. H., *J. Org. Chem.* **1993**, *58*, 7149. (e) Shinkai, S.; Minami, T.; Yoshikazu, A.; Manabe, O. *J. Chem. Soc., Perkin Trans. 2* **1985**, 503. (f) Dotsevi. G.; Cram, D. J.; Sogah, Y. *J. Am. Chem. Soc.* **1975**, 1259. (g) Chung, K. B.; Tomoi, M. *J. Polym. Sci., Part A: Polym. Chem.* **1992**, *30*, 1089. (h) Kopolow, S.; Hogen Esch, T. E.; Smide, J. *Macromolecules* **1973**, *6*, 133.

(3) For solution- and solid-phase ^{13}C NMR studies of crown ethers, see: (a) Buchanan, G. W., Gerzain, M.; Bourque, K. *Magn. Reson. Chem.* **1997**, *35*, 283. (b) Buchanan, G. W.; Driega, A. B.; Moghimi, A.; Bensimon, C.; Bourque, K. *Can. J. Chem.* **1993**, *71*, 951. (c) Buchanan, G. W.; Moghimi, A.; Ratcliffe, C. I. *Can. J. Chem.* **1996**, *74*, 1437. (d) Buchanan, G. W.; Reynolds, V. M.; Bourque, K.; Bensimon, C. *J. Chem. Soc., Perkin Trans. 2* **1995**, 707. (e) Ratcliffe, C. I.; Ripmeester, J. A.; Buchanan, G. W.; Denik, J. K. *J. Am. Chem. Soc.* **1992**, *114*, 3294. (f) Ratcliffe, C. I.; Buchanan, G. W.; Denik, J. K. *J. Am. Chem. Soc.* **1995**, *117*, 2900. (g) Buchanan, G. W.; Lefort, M.; Moghimi, A.; Bensimon, C. *J. Mol. Struct.* **1997**, 415, 267. Buchanan, G. W. *Prog. Nucl. Magn. Reson. Spectrosc.* **1999**, *34*, 327. (h) Buchanan, G. W.; Gerzain, M.; Bensimon, C.; Ellen, R.; Reynolds, V. M. *J. Mol. Struct.* **1997**, *404*, 307.

(4) Buchanan, G. W.; Driega, A. B.; Moghimi, A.; Bensimon, C.; Kirby, R. A.; Bouman, T. D. *Can. J. Chem.* **1993**, *71*, 1983.

10.1021/jo010869f CCC: $22.00
Published on Web 03/14/2002

Scheme 1. Synthesis Route for 2−6

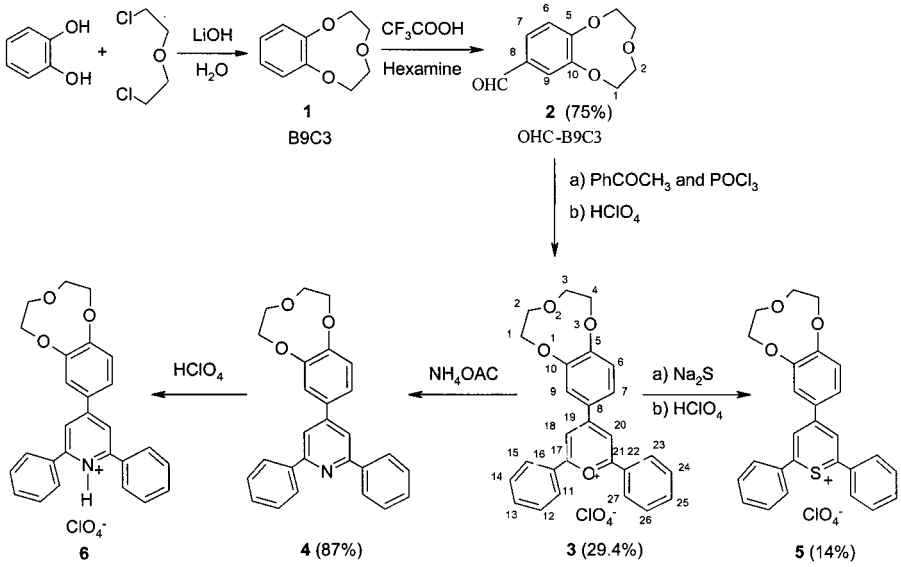

Although there are several reports on the synthesis of pyrilium, thiopyrilium, and pyridine corands,[16] as well as hemispherand-like macrocycles containing the pyrilium subunit,[17] to the best of our knowledge, there is no report on the synthesis of a molecule containing both a heteroaromatic cation and a crown ether subunit. Here, we wish to report a new class of crown ethers (compounds **3**, **5**, and **6** in Scheme 1) as pyrilium, thiopyrilium, and pyridinium crown ethers, in which a benzo-9-crown-3, B9C3,[4] unit is attached to the 2,6-diphenyl heteroaromatic cation units at the 4-position.

Since both the B9C3 and heteroaromatic cation subunits are part of a long conjugated system, any modification or change that results in the electronic changes of each of the two subunits is expected to be transformed to the other one and, consequently, change the properties of the later unit. In this article, this idea has been examined in terms of the influence of the nature of the heteroaromatic cation on the solution- and solid-phase ^{13}C NMR chemical shifts of crown ether unit. Also, the X-ray crystal structures of **3**, **4**, and **5** will be discussed. Moreover, our preliminary spectrofluoromrtric studies in methanol solution clearly revealed that the synthesized molecule **3** could be successfully used for the recognition of lysine amino acid.

Results and Discussion

Synthesis and MS. The synthetic pathway for the perchlorate salts of the target cationic molecules 2,6-diphenyl-4-B9C3-pyrilium, **3**, thiopyrilium, **5**, and pyridinium, **6**, has been shown in Scheme 1. Among a number of methods that have been suggested in the literature for the synthesis of pyrilium and thiopyrilium cations,[16−21] the method shown in Scheme 1 was chosen in order to prepare both thiopyrilium and pyridinium derivatives from the pyrilium cation.

The pyrilium salt **3** was obtained in three steps from catechol as follows. B9C3 was synthesized following a procedure described before.[4] In the second step, B9C3 was formylated with hexamine in the presence of CF_3COOH to obtain crystalline 4′-HCO-B9C3, **2**, in a yield of 75%.

(5) (a) Gokel, G. W.; Korzeniowski, S. H. *Macrocyclic Polyether Synthesis*; Springer: Berlin, 1982. (b) Bradshaw, J. S.; Krakowiak, K. E.; Izatt, R. M.; Bruening, R. L.; Tarbet, B. J. *J. Heterocycl. Chem.* **1990**, *27*(2), 347. (c) Pedersen, E. J.; Bradshaw, J. S. In *Synthetic Multidentate Macrocyclic Compounds*; Izatt, R. M., Christensen, J. J., Eds.; Academic Press: New York, 1978; pp 1−111. (d) Gokel, G. *Crown Ethers and Cryptands*; Royal Society of Chemistry: Cambridge, 1991; pp 22−36.

(6) Weissenfels, M.; Pulst, M.; Greif, D. *Sulfur Rep.* **1993**, *15*, 161.

(7) Kuthan, *J. Adv. Heterocycl. Chem.* **1983**, *34*, 145.

(8) Kuthan, J.; Sebek, P.; Bohm, S. *Adv. Heterocycl. Chem.* **1994**, *59*, 179.

(9) Doddi, G.; Ekcolani, G. *Adv. Heterocycl. Chem.* **1994**, *60*, 65.

(10) (a) Krivun, S. V.; Baranov, S. N.; Buryak, A. I. *Khim. Geterotsikl. Soedim.* **1971**, *7*(10), 132. (b) CA, 57:026678, Jpn. Kokai Tokkyo Koho JP82 26,678; CA 114:143078q; CA 115:183033y; CA 119:282020f; CA 78:29545c.

(11) Izatt, R. M.; Clark, G. A.; Bradshaw, J. S.; Lamb, J. D.; Christensen, J. J. *Sep. Purif. Methods* **1986**, *15*, 21. (b) Kimura, K.; Shano, T. In *Cation Binding by Macrocycles*; Inoue, Y., Gokel, G. W., Eds.; Marcel Dekker: New York, 1990. (c) Dozol, M. In *New Separation Chemistry Techniques for Radioactive Waste and Other Specific Applications*; Cecille, L., Casaraci, M., Pietrelli, L., Eds.; Elsevier: Amsterdam, 1991. (d) Visser, H. C.; Reinhoudt, D. N.; de Jong, F. *Chem. Soc. Rev.* **1994**, 78.

(12) (a) Arnold, M. A.; Meyerhoff, M. E. *Crit. Rev. Anal. Chem.* **1988**, *20*, 149. (b) Bulhmann, P.; Pretsch, E.; Bakker, E. *Chem. Rev.* **1998**, *98*, 1593. (c) Gangali, M. R.; Rouhollahi, A.; Mardan, A. R.; Hamzeloo, M.; Moghimi, A.; Shamsipur M. *Microchem. J.* **1998**, *60*, 122. (d) Gangali, M. R.; Moghimi A.; Shamsipur, M. *Anal. Chem.* **1998**, *70*, 5259. (e) Rouhollahi, M. R.; Gangali, A. Moghimi, A.; Buchanan, G. W.; Shamsipur, M. *J. Inclusion Phenom.* **1998**, *70*, 5259.

(13) Moore, J. A.; Partain, E. M. In *Crown Ether and Phase Transfer Catalysis in Polymer Science*; Mathias, L. J., Carraher, C. E., Jr., Eds.; Plenum Press: New York, 1984; p 291.

(14) (a) Teegarden, D. M.; Herkstoreter, W. G.; McColgin, W. C. *J. Imaging Sci. Technol.* **1993**, *37*(2), 149. (b) Detty, M. R.; Merkel, P. B. *J. Am. Chem. Soc.* **1990**, *112*, 3845. (c) Detty, M. R.; Gibson, S. L. *Organometallics* **1992**, *11*, 2147. (d) Borsenberger, P. M.; Hoesterey, D. C. *J. Appl. Phys.* **1980**, *51*, 4248. (e) Iwata, K.; Hagiwara, T.; Matsuzawa, H. *J. Polym. Sci. Polym. Chem. Ed.* **1986**, *24*, 1043.

(15) JP 8226,678; JP 01-126,655; GE 3832940; JP 63-303362; GE 3832903; GE 3630389; JP 59-146061; US 4384034; US 4368329; JP 01-126655; JP 63-13792; EU 319296; US 5019549; US 4125414.

(16) (a) Doddi, G.; Ercolani, G.; Mencarelli, P. *Tetrahedron* **1991**, *47*, 10/11, 1977. (b) Eisner, U.; Krishnamurthy, T. *J. Org. Chem.* **1972**, *37*, 150.

(17) (a) Dijkstra, P. J.; den Hertog, H. J., Jr.; van Eerden, J.; Harkema, S.; Reinhoudt, D. N. *J. Org. Chem.* **1988**, *53*, 374. (b) Dijkstra, P. J.; den Hertog, H. J., Jr.; van Steen, B. J.; Hams, B. H. M.; Reinhoudt, D. N. *Tetrahedron Lett.* **1986**, *27*, 3183.

(18) Doddi, G.; Ercolani, G.; Nunziante, P. *J Chem. Soc. Perkin Trans. 2* **1987**, 1427.

(19) (a) Wizinger, R.; Ulrich, P. *Helv. Chim. Acta* **1956**, *39*, 207.

(20) Maryanoff, B. E.; Stackhouse, J.; Senkler, G. H.; Mislow, K. *J. Am. Chem. Soc.* **1975**, *97*, 2718.

(21) (a) Wizinger, R.; Losinger, S.; Ulrich, P. *Helv. Chim. Acta* **1956**, *39*, 5. (b) JP 82 26,678.

The third step reaction was carried out using 1 mol of **2** and 2 mol of acetophenone in the presence of $POCl_3$. This procedure was taken from a report presented by Wizinger et al. a long time ago.[19] Thus, the first pyrilium crown ether, **3**, which decomposes at about 250 °C, was obtained in 29% yield.

To replace the O^+ heteroatom of **3** with an N atom, a normally used procedure[9,16] for the pyrilium to pyridine transformation was applied, providing some minor modification in the work up. On the basis of this procedure, the pyrilium salt, **3**, was reacted with ammonium acetate in glacial acetic acid and the resulting crude product was recrystalized from ethanol to obtain a colorless cubic crystalline product, **4**, in 80% yield. The pyridine derivative transformation to its protonated cationic counterpart, **6**, was performed via addition of $HClO_4$ to an acetonitrile solution of **4**.

To convert the pyrilium salt **3** to the corresponding thiopyrilium derivative, in a separate experiment the compound **3** was reacted with Na_2S followed by treatment with 20% $HClO_4$ in order to get the perchlorate **5** in 14% yield. The ^1H NMR spectrum of the crude sample obtained indicated that the starting material **3** was present to an extent of ca. 8%. The crude sample thus obtained was again treated with Na_2S two more times, using the same procedure as before, and the final product was recrystalized from CH_2Cl_2/Et_2O to get pure product, as determined by ^1H NMR. It is believed[19] that the pyrilium to thiopyrilium transformation proceeds through the formation of an acyclic keto-thioenolate anion as an intermediate that undergoes cyclization to the final thiopyrilium cation after acidification.

Doddi et al.[22] have noted that the EI condition in mass spectroscopy is not a proper technique for structural characterization of organic salts such as heteroaromatic cations. Low volatility and thermal degradation are in fact two limiting factors under such condition. This was checked on **3** at a 70 eV field; the resulting spectrum featured a base peak at 109.0. A search in the literature showed that the FAB-MS method has been successfully applied for 39 of such compounds by Doddi et al.[23] Moreover, the ESI-MS was another potential choice that has not been applied to this class of organic salts previously. In this work we employed the ESI-MS method in order to get more satisfactory information for the structural characterization of the ligands synthesized. The positive ESI-MS has recently been applied to a number of complicated large size molecules.[24] In the ESI-MS spectrum of **3**, using CH_3OH as carrier, the base peak was found to be $m/z = 411.0$ corresponding to the naked cation, 2,6-diphenyl-4-B9C3 pyrilium $C_{27}H_{23}O_4^+$. The ESI-MS and elemental analysis data were found to be reasonably in support of the expected structure for compound **3**.

For the pyridine derivative **4**, both EI-MS and ESI-MS techniques were informative. The resulting M^+ peak in EI mode was matched for exact mass of **4**; calcd 409.1678, found 409.1681. The ESI mode in two different carriers HCOOH and CH_3OH + KCl was also checked.

Table 1. UV-Vis Data for 3−6

compound	solvent	absorptions (nm)			
3	EtOH	206	238	277	422
	CH_3CN	201	237	275	413
5	CH_3CN	200		271	413
	EtOH	207		270	413
4	CH_3CN	211	233	269	
	EtOH	211	233	269	
6	CH_3CN	211	233	269	350

The proper M + 1 and $(M + K)^+$ peaks, which are good signs for the structural elucidation, were detected.

Two samples (I) and (II) for thiopyrilium derivative **5** were obtained. Successive treatment of the crude product with Na_2S was performed to purify sample I. It is very difficult to get rid of **3** as impurity in **5** because both compounds recrystalize simultaneously. To check the impurity in samples I and II, the ESI-MS was run on both. The sample I showed both **3** and **5** in 50:100 peak intensity ratio, and that for sample II was 5:100. The results thus obtained ratified the effectiveness of the methodology applied to obtain the sample II with much lower amount of **3** as impurity. However, the sample sent for the X-ray crystal structure determination showed the presence of trace amount of 3 in **5**.

UV−Vis Spectroscopy. The pyrilium and thiopyrilium cations **3** and **5** in EtOH and CH_3CN as solvent are reddish orange. The UV−vis data for **3**−**6** are collected in Table 1. The most important feature of the data presented in Table 1 is the significant change occurred for the λ_{max} of **4** once it is protonated. Upon protonation of **4**, the number of absorptions is increased from three, in **4**, to four, in **5**; the new band in **5** (i.e., 350 nm) being shifted to longer wavelengths for some 81 nm in comparison with the longest absorption in **4** (i.e., 269.4 nm). This is an indication of the expansion of the conjugated system when protonation takes place. Change in the solvent from EtOH to CH_3CN resulted in a blue shift for **3**, whereas **4** was not much affected by the solvent properties. The present pyrilium cation is close, in its longest-wavelength absorption maxima (350 nm), to a number of examples reported in the literature,[25] including 4-anisyl-2,6-diphenyl, 2,4-dianisyl-6-phenyl, 2,4,6-trianisyl, and 2,6-dianisyl-4-(3,4-dimethoxyphenyl) pyrilium perchlorates whose λ_{max} are located at 418, 416, 420, and 423, respectively.

The second feature of the UV data is the similarities between pyrilium and thiopyrilium cations **3** and **5**. The closest example, in structure, in the literature is 2,6-bis (methoxyphenyl)-4-(3,4-dimethoxyphenyl)-pyrilium perchlorate with a λ_{max} in CH_3CN at 423 nm.[21] The solvent effect on λ_{max} of the pyrilium and thiopyrilium derivatives has been explained by Saeva et al. in terms of the influence of solvent dielectric constant on the ground and excited states.[26]

Solution ^1H and ^{13}C NMR. The solution ^1H NMR spectrum of **3** shows three mutiplets in the 4.3−4.9 ppm region and a specific pattern for three protons of the 4′-substituted-B9C3 benzene ring. The two equal pyrilium protons at 18 and 20 positions show a well-separated singlet signal at 8.5 ppm. These two protons are equal because of the fast B9C3 rotation, in the NMR time scale, about the C−C bond that connects the two units to each other.

(22) Cordischi, V. C.; Doddi, G.; Stegel, F. *J. Org. Chem.* **1982**, *47*, 3496.
(23) De Angelis, F.; Doddi, G.; Ercolani G. *J. Chem. Soc., Perkin Trans. 1* **1987**, 633.
(24) Cotton, R.; D'Agostino, A.; Traeger, J. C. *Mass Spectrosc. Rev.* **1995**, *14*, 79.
(25) Bersani, S.; Doddi, G.; Fornarini, S.; Stegel, F. *J. Org. Chem.* **1978**, *43*, 4112.
(26) Saeva, F. D.; Olin, G. R. *J. Am. Chem. Soc.* **1980**, *102*, 299.

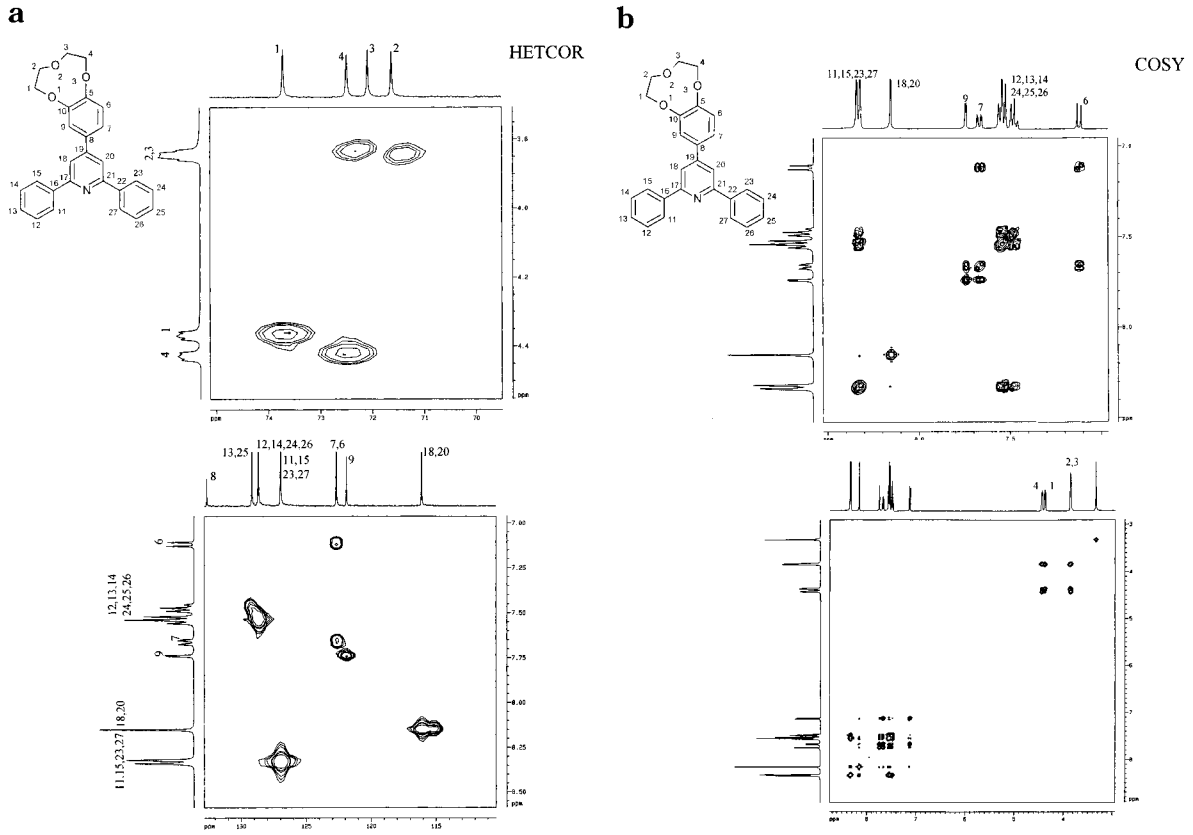

Figure 1. (a) Two-dimensional $^1H-^{13}C$ HETCOR and (b) $^1H-^1H$ COSY for **4**.

The solution ^1H resonances of **5** are more or less similar to those observed for **3**. From the ^1H spectral analysis of **4** it becomes apparent that **4** behaves a little differently from **3** and **5**. A notable difference is the number of multiplet peaks for -CH_2O- protons of the crown cavity. The compounds **3** and **5** show three of such mutiplets, whereas **4** exhibits two. This is a result of electron-withdrawing character of the pyrilium and thiopyrilium cation units in comparison to the pyridine. A similar effect has already been reported for HCO-B9C3[27] and NO_2-B9C3.[28] The remote electronic effect of pyrilium and thiopyrilium units is in fact tansferred to the B9C3. Therefore, the average conformation of the nine-membered ring crown cavity is changed. Therefore, the -CH_2O- resonances at 1- and 4-positions are well separated.

The solution ^{13}C NMR spectra of **3**, **4**, and **5** were analyzed on the basis of the previously resolved ^{13}C NMR spectrum of NO_2-B9C3,[28] the ^{13}C NMR data of **2**,[27] the two-dimensional $^1H-^1H$ COSY for **3** and **4**, and the two-dimensional $^1H-^{13}C$ HETCOR for **4**. The typical two-dimensional spectra of **4** are shown in Figures 1a and 1b. The three aromatic CH protons of B9C3 in ^1H NMR spectra give rise to two d and one dd patterns, which can be easily analyzed. The cross-peaks observed in the COSY, as shown in Figure 1b further supported the assignment of these protons. The ^1J HETCOR experiment furnished assignments of the directly bonded carbons to H6, H7, and H9. On the basis of the known singlet signal for H18 and H20, the assignment of C18 and C20 was straightforward from HETCOR. The H18 and H20 peaks of **3** and **5** appeared at 9.0 and 9.2 ppm, respectively. This is in accordance with the previous observations that the β protons in 2,4,6-triphenylpyriliums and thiopyriliums normally appear as a singlet at about 9 ppm.[18,20,22,29] The compound 2,4,6-triphenyl thiopyrilium, for example, has been reported to exhibit a singlet ^1H NMR peak for the two β protons at 9.3, 9.2, and 9.1 ppm in DMSO-d_6, CD_3-OD, and CD_3CN solvents, respectively.[22,30] Cosy experiments were also informative in the assignment of the CH_2O protons. Subsequent HETCOR experiments aided in identification of corresponding bonded carbons.

A great chemical shift difference is observed for C19 and C17 in **3** and **5** in one hand and **4** on the other hand. These $\Delta\delta$C are 17.6 and 6.3 ppm for the **3** and **4** couple and 12.9 and 10.6 ppm for the **5** and **4** couple, respectively. The low field shift of these two carbons is mainly due to the inductive effect of positively charged O^+ and S^+ centers.

The most interesting issue to be investigated, in this section, is the influence of the B9C3 crown ring on the heteroaromatic unit and vice versa by NMR spectroscopy. To perform an estimation of the contribution of the B9C3 crown ring on the ^{13}C NMR resonances of pyrilium unit in **3**, the compound 2,4,6-triphenyl pyrilium perchlorate was synthesized. The chemical shifts of the C18 and C20 carbons in this compound were found to be 115.0 ppm in DMSO-d_6 solvent. This test simply indicates that there is 1.6 ppm ^{13}C shielding effect arising from the resonance effect of the *para* O3 oxygen. The tertiary C17 and C19 carbons in this compound were found to be 169.9 and

(27) Buchanan, G. W.; Rastegar, M. F.; Yap, G. P. A. *J. Mol. Struct.* **2001**, *561*, 43.
(28) Buchanan, G. W.; Driega, A. B.; Moghimi. A.; Bensimon, C. *Can. J. Chem.* **1994**, *72*, 1764.
(29) Desbene, P.-L.; Cherton, J.-C.; LeRoux J.-P.; Basselier, J.-J. *Tetrahedron* **1984**, *40*, 3539.
(30) Doddi, G.; Ercolani, G. *J. Chem. Soc., Perkin Trans. 1* **1988**, 271.

Table 2. Crystal Data and Structure Refinement for 3−5

	3	**5**	**4**
empirical formula	$C_{27}H_{23}NO_3$	$C_{27}H_{22}ClO_8$	$C_{27}H_{23}ClO_7S$
wavelength (Å)	0.71073	0.71073	0.71073
crystal system	orthorhombic	monoclinic	orthorhombic
space group	P2 (1) 2 (1) 2 (1)	P2 (1)	P2 (1) 2 (1) 2 (1)
a (Å)	7.5521 (6)	11.104 (1)	7.721 (3)
b (Å)	15.574 (1)	7.337 (2)	15.488 (6)
c (Å)	20.024 (2)	13.303 (1)	19.704 (7)
α, β, γ	90, 90, 90	90, 108.737 (2)	90, 90, 90
volume (Å^3)	2355.2 (3)	1026.3 (2)	2356.2 (2)
Z (atoms/unit cell)	4	2	4
calcd density (gm/cm^3)	1.438	1.325	1.451
reflections collected	18501	6553	18605
unique	5681 [R (int) = 0.0616]	2293 [R (int) = 0.0438]	2471 [R (int) = 0.2851]
F (0 0 0)	1060	432	1071
crystal size	0.4 × 0.4 × 0.4 mm^3	0.4 × 0.3 × 0.2 mm^3	0.2 × 0.1 × 0.1 mm^3
θ range (deg)	1.66 to 28.74	1.62 to 23.25	1.67 to 20.81
limiting indices	h (−10 to 10)	h (−12 to 11)	h (−7 to 7)
	k (0 to 20)	k (−4 to 8)	k (0 to 15)
	l (0 to 27)	l (0 to 14)	l (0 to 19)
goodness-of-fit on F^2	1.014	1.030	1.079
final R indices [$I > 2\sigma(I)$]	R1 =0.0509, wR2 =0.1149	R1 =0.0572, wR2 =0.1673	R1 =0.0762, wR2 =0.1915
R indices (all data)	R1 =0.0666, wR2 =0.1177	R1 =0.0683, wR2 = 0.1923	R1 =0.0876, wR2 =0.2023
absolute structure parameter	0.04 (7)	0.037 (9)	0.08 (2)
largest diff. peak and hole (e/Å^3	0.358 and −0.432	0.258 and −0.218	0.300 and −0.609

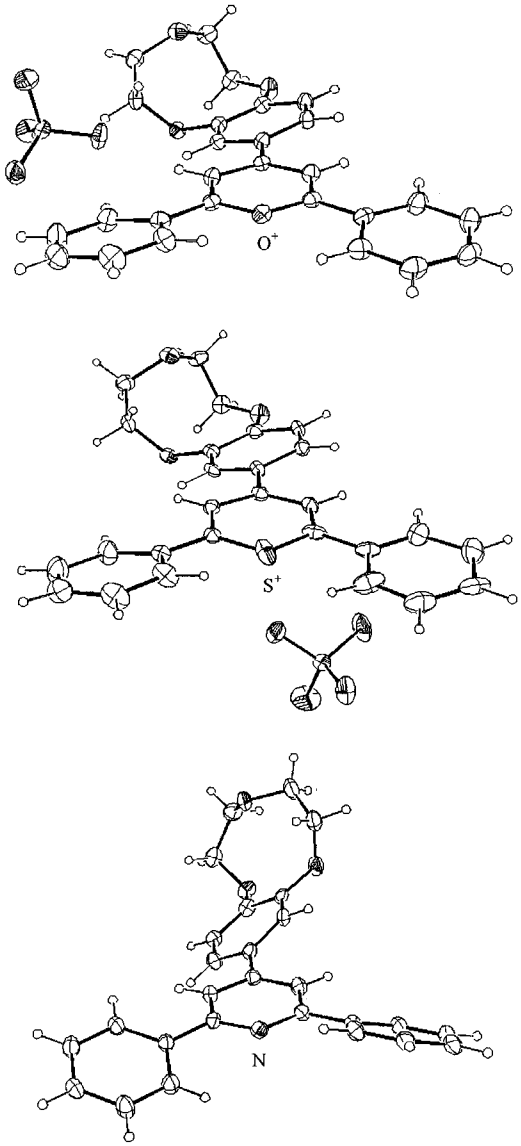

Figure 2. ORTEP diagrams for **3**, **4**, and **5**.

164.9 ppm, respectively, in DMSO-d_6. This means that these two carbons in **3** are 1 and 1.9 ppm, respectively, more shielded than the corresponding carbons in the 2,4,6-triphenyl pyrilium perchlorate. As seen, B9C3 crown ring affects electronically the heteroaromatic ring.

The nature of the unit connected to the benzene ring of B9C3 could also change the properties of the crown ether unit. An important point to be noticed, in this regard, is the similarities between the solution ^{13}C NMR data of **2**, **3**, and **5**, on one hand, and their differences from those of **4**, on the other. The B9C3 and heteroaromatic cation or formyl units in the former three cases are electronically complementary from the electron donation and acceptance point of view. The formyl, pyrilium and thiopyrilium units induce deshielding on most of the ^{13}C resonances of the B9C3 fragment in **2**, **3**, and **5** respectively. Investigation of the ^{13}C NMR data of the present three B9C3 derivatives and **2**[27] reveals that the chemical shift difference between the C5 and C10 signals in **2**, **3**, and **5** is 5.6, 6.3, and 5.7 ppm, respectively, while it is only 0.8 ppm in the case of **4**. This is because of the partial positive charge induced by the CHO, O^+, and S^+ groups through resonance effect. As expected and previously observed in **2**, C4 in the compounds **3** and **5** is more shielded than C1, although the pyrilium and thiopyrilium units as electron-withdrawing groups are located at the *para* position to the B9C3 benzene ring. The chemical shift of C4 and C1 is dependent, in fact, on the C6−C5−O3−C4 and C9−C10−O1−C1 torsion angles.

X-ray Crystal Structures. The ORTEP diagrams for **3**, **4**, and **5** are shown in Figure 2, and the corresponding crystal structure data are presented in Table 2. Moreover, some selected bond lengths, bond angles, and torsion angles data are collected in Table 3. The previously reported X-ray crystal structure data of **2**[27] are also included in Table 3 for comparison.

An overall comparison indicates that the two electron-withdrawing substitution groups 2,6-diphenyl pyrilium (in **3**) and 2,6-diphenyl thiopyrilium (in **5**) at the 4′-position to the B9C3 behave remarkably the same as the formyl, HCO, group in **2**. Interestingly, the data for **2**, **3**, and **5** are different from those of **4,** and the stereochemistry of crown ring in B9C3 is dependent on the nature of 4′-substitution group. A comparison between the nine-membered ring torsion angles in **2**, **3**, **4**, and **5** indicates that there is a great difference between the two C4−O3−

Table 3. Comparison of Selected Bond Lengths (Å), Bond Angles and Torsion Angles (deg) in 2−5

	3	5	4	2
C9−C10−O1−C1	71.3	73.8	−75.1	73.7
C10−O1−C1−C2	101.4	103.4	−98.8	103.4
O1−C1−C2−O2	−61.0	−62.8	65.3	61.3
C1−C2−O2−C3	114.2	113.8	−120.5	112.3
C2−O2−C3−C4	−71.7	−70.8	122.2	73.8
O2−C3−C4−O3	−68.8	−69.3	−68.2	66.3
C3−C4−O3−C5	78.6	79.2	99.1	87.0
C4−O3−C5−C6	−168.8	−166.6	75.9	175.3
C7−C8−C19−C20	−12.7	−12.6	−31.8	
C20−C21−C22−C23	2	5.2	−19.7	
C18−C17−C16−C15	11.5	13.4	−26.2	
C5−O3−C4	124.44	125.80	115.24	123.91
C10−O1−C1	115.41	114.51	115.84	114.81
C5−O3	1.354	1.358	1.404	1.358
C8−C19	1.460	1.478	1.505	
C21−C22	1.464	1.459	1.488	
C17−C16	1.466	1.466	1.474	

C5−C6 and C2−O2−C3−C4 networks of **2**, **3**, and **5** compounds and **4**; the absolute values of the former torsion angle range from 175.3° to 166.6° in **2**, **3**, and **5** while it is 75.9° in **4**, whereas the absolute values for the later torsion angles range from 70.8° to 73.4° in **2**, **3**, and in **5** while it is 122.2° in **4**. In a recent publication on 4′-substituted B9C3 derivatives, it has been concluded that there is little conformational effect of the aromatic substitution on the crown ether.[27] Such conclusion has been deduced from the comparison of the NMR data of B9C3 and its derivatives containing electron-withdrawing groups CHO, COMe, COOH, and NO_2.

In addition to the 4′-substitution, the crystal packing can also change the stereochemistry of the crown ring in B9C3 derivatives. A known example of this factor is a recently published paper on tris(9-crown-3) triphenylene[31] in which the stereochemistry of three nine-membered crown rings differ from each other. However, the influence of the anionic counterion ClO_4^- is not the origin of the discussed differences since such differences exist between **2** and **4** also. Moreover, if the ClO_4^- counterion had a considerable contribution on the determination of the stereochemistry of the crown ring, then one would have expected to observe enormous structural differences between **3** and **5** because of the noticeable positional difference for ClO_4^-.

Another interesting feature of the geometries of **3** and **5** is the coplanarity observed between the four aromatic rings. Three key torsion angles that clearly determine the deviation of aromatic rings from coplanarity for **3**, **4**, and **5** are given in Table 3. The most pronounced deviation was found in the case of **4**. Compounds **3** and **5**, again, show very close similarities in this regard. As presented, the smallest deviation from planarity occurs in the C20−C21−C22−C23 network where the torsion angle is 2.0° and 5.2° in **3** and **5,** respectively. Thus, it can be concluded that the heteroaromatic cation rings are the origin of the coplanarity existing among the four aromatic rings in **3** and **5**.

The location of the ClO_4^- anion in **3** and **5** is another interesting issue that needs some explanation. The ORTEP diagrams of **3** and **5** reveal that the large size ClO_4^- anion can be accommodated in the space provided between to 2,6-phenyl rings of **5** beside the S^+ center, while such situation does not exist for **3**. It is of interest to note that the distance S···Cl in **5** is 3.000 Å, while the O···Cl distance in **3** is 6.607 Å. Since there is a little difference between the C20−C21−C22−C27 and C18−C17−C16−C11 torsion angles in **3** and **5**, the differentiation of anion accommodation could be due to the polarizability of S^+ and its larger size.

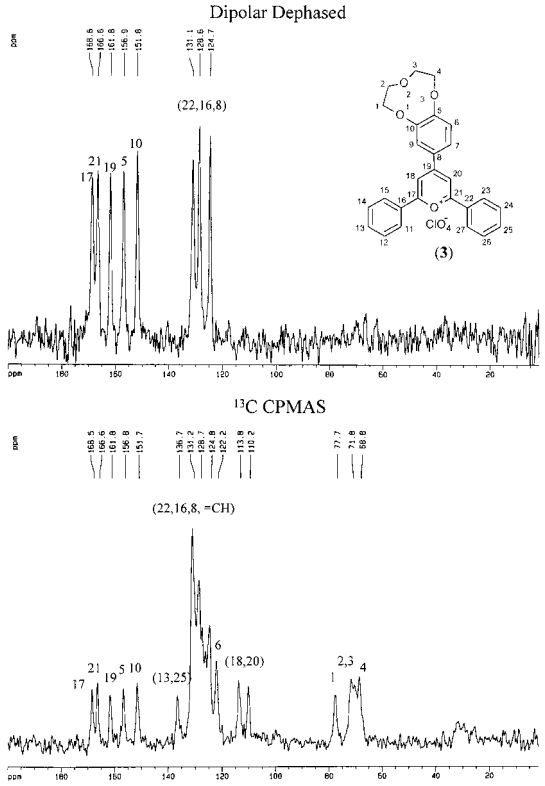

Figure 3. Normal and dipolar dephased ^{13}C NMR of solid **3**.

The final structural feature worth mentioning is the difference between some of the bond lengths and angles given in Table 3. The C5−O3 bond, *para* to 4′-substitution, is almost the same in **3** and **5** (1.354 and 1.358 Å), respectively, while quite different from that in **4** (i.e., 1.404 Å). This is most possibly a result of the long conjugation system formed between the O3−C5 bond, the B9C3 benzene ring, the heteroaromatic cation ring, and the two phenyl rings attached to the central heteroaromatic ring. It is for this reason that the bond length C8−C19 in **3** and **5** are shorter than the corresponding bond length in **4**. Interestingly, the bonds that connect two phenyl groups to the heteroaromatic ring in **3** and **5** are different in lengths. The smaller C21−C22 bond connects the more planar phenyl ring to the heteroaromatic ring.

Solid-Phase ^{13}C NMR. The normal and dipolar dephased solid phase ^{13}C NMR spectra of **3**, **4**, and **5** are presented in Figures 3−5. The selected ^{13}C solid-phase NMR data for **3**, **4**, and **5** are collected and compared to the corresponding ^{13}C NMR data of **2** in Table 4.

An overall look at the three ^{13}C CPMAS spectra reveals three distinct regions: a 68−79 ppm region for crown cavity -CH_2O- carbons, a low field region of 150−169 ppm for C5, C10, C19, C17, and a 110−137 ppm region for the remaining, mostly CH, carbons. The full analysis of ^{13}C CPMAS spectra may not be performed because of the peak overlapping, particularly in the 110−137 ppm region, and the lack of enough data for this purpose. The present analysis was carried out on the basis of the previously analyzed ^{13}C CPMAS data for B9C3 and

(31) Buchanan, G. W.; Rastegar, M. F.; Yap, G. P. A. *Can. J. Chem.* **2001**, *79*, 195.

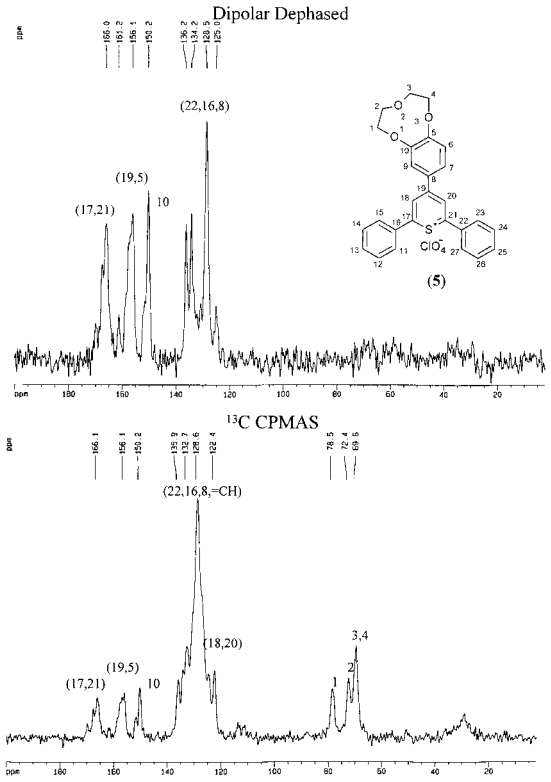

Figure 4. Normal and dipolar dephased ^{13}C NMR of solid **5**.

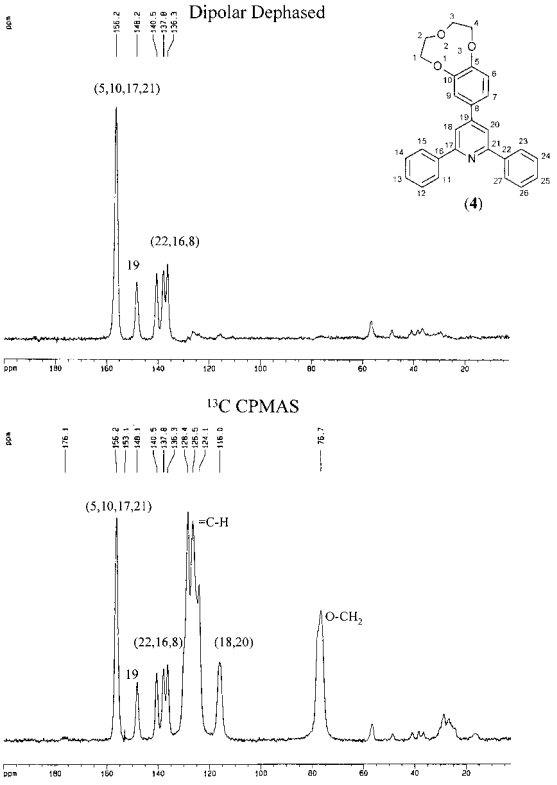

Figure 5. Normal and dipolar dephased ^{13}C NMR of solid **4**.

B9C3-d_4,[4] and for 4′-HCO-B9C3 and 4′-HCO-B9C3-d_4,[27] present dipolar dephased ^{13}C CPMAS spectra, logical factors influencing δC, and finally, the solution ^{13}C NMR data.

There is a remarkable similarity between the pattern and chemical shift dispersion of ethereal carbons, -CH_2O-, in **2**, **3**, and **5**, while the corresponding carbons in **4** show only one broadened singlet signal at 76.7 ppm. The most deshielded resonance in the aliphatic -CH_2O- region corresponds to C1. The substantial chemical shift difference between C1 and C4 is essentially constant in **2**, **3**, and **5** with an average value of 8.7 ± 0.5 ppm. The dependence of the total shielding of -OCH_2- carbons connected to the B9C3 has been shown to be aryl−O−CH_2− torsion angle dependent.[4] The average value of C9−C10−O1−C1 and C6−C5−O3−C4 torsion angles given in Table 3 for **2**, **3**, and **5** are 73 ± 2° and 170 ± 4°, respectively, and the corresponding angles in **4** are 75.1° and 75.9°, respectively. For this reason, the chemical shifts of C1 and C4 in **4** are very close to each other (76.7 ppm), while those of the same carbons in **2**, **3**, and **5** are 78 ± 1 and 69 ± 1 ppm, respectively.

Table 4. Selected Resolved ^{13}C Resonances in the Solid-Phase NMR Spectra of 2−5 (δc from TMS ± 0.1)'

carbon	3	5	4	2
C1	77.7	78.5	76.7	77.6
(C2, C3)*	71.8, 70.5	72.4, 69.5	76.7	73.8
C4	68.8	69.5	76.7	69.3
C5	156.9	157.0	156.2	157.7
C6	122.2			122.4
C10	151.8	150.2	150.2	150.2
(C8, C16, C22)[a]	131.1, 128.6, 124.7	136.2, 134.2, 128.5	140.5, 137.8, 136.3	131.9
(C17, C21)[a]	168.6, 166.6	167.0, 166.0	156.2	
(C18, C20)[a]	113.8, 110.2	122.4, 125.0	−116.0	
C19	161.8	162.0	148.2	

[a] May be interchanged.

The eight quaternary carbons in **3**, **4**, and **5** are clearly evident in the dipolar dephased ^{13}C CPMAS spectra (Figures 3−5). This multiplicity in the solid-state spectra is consistent with the lack of symmetry in the X-ray crystal structure. The aromatic carbons, C5, C10, C17, and C21, which are connected to either O or N atoms as well as C19 carbon in heteroaromatic rings, are the most deshielded aromatic carbons.

It is noteworthy that the $\Delta\delta$C values for C5 and C10 in **3** and **4** are 5.1 and 0 ppm, respectively. The zero differentiation is most probably a result of the similarities between C10−C5−O3−C4 and C5−C10−O1−C1 torsion angles and the lack of a strong electron-withdrawing group at 4′-position of B9C3 in **4**. These two factors are totally different in **3**. and therefore, a 5.1 ppm shift difference is observed for this compound.

The degree of planarity existing between the 2,6-diphenyl and heteroaromatic cation rings is one of the factors that are expected to influence the ^{13}C shielding of the aromatic C18 and C20 carbons. As noted before, these two carbons show one signal in the solution ^{13}C NMR spectrum. In the solid phase, however, this single signal has been doubled since these two carbons are not equal anymore. The ^{13}C chemical shift difference for this couple in **3** is 3.6 ppm. More deviation from planarity reduces the steric interactions between H23 and H20 or H15 and H18, resulting in less shielded C18 and C20 carbons. An investigation of the two torsion angles C20−C21−C22−C23 and C18−C17−C16−C15 in **3** (2° and 11.5°, respectively) indicates that there is more steric interaction between H23 and H20 in this case, which results in less shielding for C18 over C20.

Amino Acid Recognition in Methanol Solution. In neutral protic solvents, amino acids exist largely as strongly solvated zwitterionic structure. The electronic densities at the carboxylate and ammonium functions are

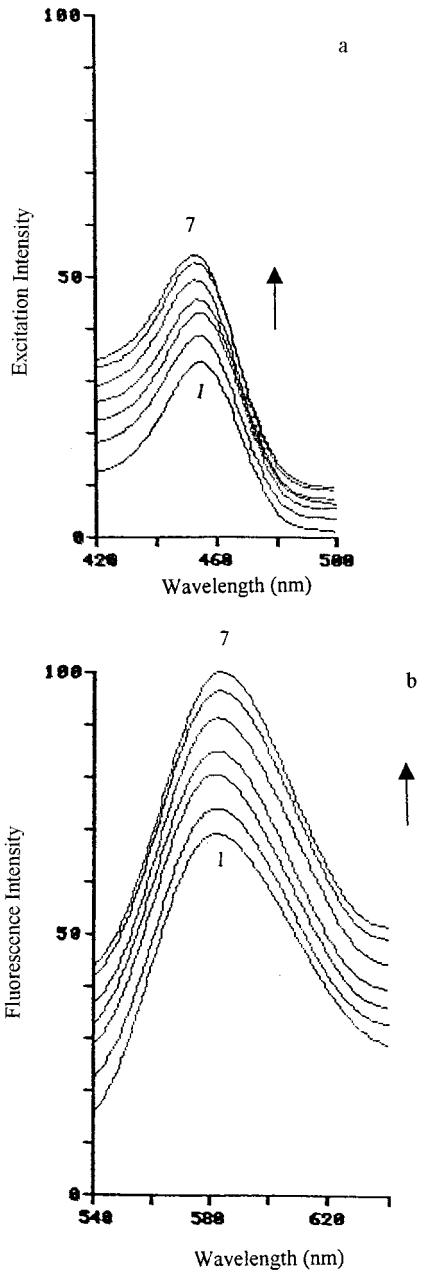

Figure 6. Excitation (a) and emission (b) spectra of a fixed concentration of **3** (1.00×10^{-6} M) in methanol in the presence of increasing concentration of lysine: (1) 0.0, (2) 8.3×10^{-5} M, (3) 1.67×10^{-4} M, (4) 2.50×10^{-4} M, (5) 3.33×10^{-4} M, (6) 4.12×10^{-4} M, (7) 4.97×10^{-4} M.

greatly affected by their mutual vicinity, causing the binding forces of complementary groups of the receptor to be less effective for the complexation. Thus, the design of a model receptor for specific amino acids in zwitterionic form is still a challenging problem.[32−34]

The compound **3**, which contains nonself-complementary binding site for carboxylate (a pyrilium function) and ammonium (a crown ether), is expected to act as a suitable receptor for specific amino acids. Thus, the possibility of the interaction of several amino acids

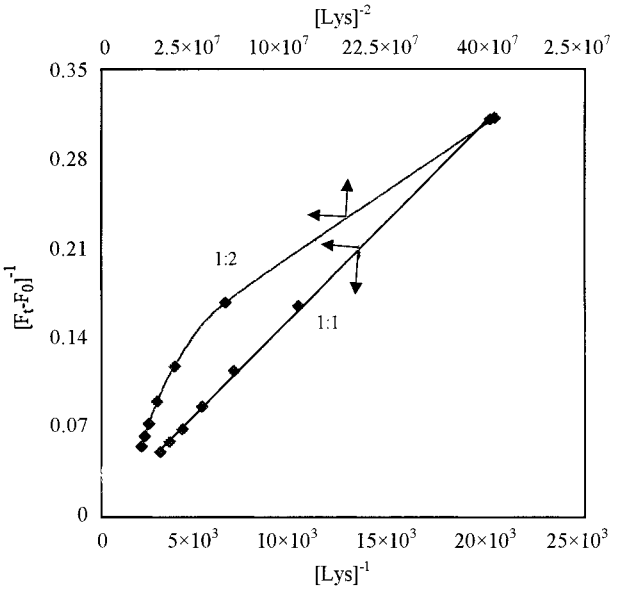

Figure 7. Plots of (a) $1/(F_t - F_o)$ vs $1/[\text{Lys}]_o$ and (b) $1/(F_t - F_o)$ vs $1/[\text{Lys}]_o^2$ for the lysine-**3** complexation.

including histidine, serine, argenine, cystein, glycine, leucine, and lysine was examined using a spectrofluorometric technique. Among these amino acids lysine was found to selectively bind to the receptor molecule **3**.

The excitation and emission spectra of **3** (1.0×10^{-6} M) in the presence of increasing excess amount of lysine are shown in Figure 6. To evaluate the stoichiometry and stability constant, K_s, of the complex formed between the amino acid and receptor **3**, the fluorescence intensity vs lysine concentration data were fitted to the linear equations 1 and 2, derived for 1:1 and 2:1 (amino acid: receptor) stoichiometries, respectively:[35, 36]

$$\frac{1}{F_t - F_o} = \frac{1}{(F_b - F_o)K_s[\text{Lys}]_o} + \frac{1}{F_b - F_o} \qquad (1)$$

$$\frac{1}{F_t - F_o} = \frac{1}{(F_b - F_o)K_s[\text{Lys}]_o^2} + \frac{1}{F_b - F_o} \qquad (2)$$

where F_t, F_b, F_o, and $[\text{Lys}]_o$ denote the observed fluorescence intensity, fluorescence intensity of **3** when totally bonded to lysine, initial fluorescence intensity of **3** in the absence of amino acid, and total lysine concentration, respectively. The resulting plots of $1/(F_t - F_o)$ vs $1/[\text{Lys}]_o$ (a) and $1/(F_t - F_o)$ vs $1/[\text{Lys}]^2_o$ (b) are shown in Figure 7. As is immediately obvious, the best linear fit was obtained for the 1:1 stoichiometry, while the use of a 2:1 model resulted in a distinct deviation from the expected linear behavior. The average K_s value obtained from six series of repeated experiments was found to be $K_s = 265 \pm 33$, while the K_s value for the leucine-**3** system was found to be <10.

A comparison between the results obtained for lysine (as a both α−α and α−ω amino acid) and those with leucine (as an α−α amino acid) clearly indicates that the simultaneous interaction of the α-amino (with the crown ring of **3**) and ω-carboxylate groups (with the positively charged pyrilium oxygen of **3**) resulted in a fairly stable

(32) Schmidtchen, F. P. *Tetrahedron Lett.* **1984**, *25*, 4361.
(33) Kimura, E.; Fujioka, H.; Kodoma, M. *J. Chem. Soc., Chem. Commun.* **1986**, 1158.
(34) Hossain, M. A.; Schneider, H.-J. *J. Am. Chem. Soc.* **1998**, *120*, 11208.
(35) Eddaondi, M.; Coleman, A. W.; Prognon, P.; Lopez-Mahia, P. *J. Chem. Soc., Perkin Trans. 2* **1996**, 955.
(36) Pistotis, G.; Malliaris, G. *J. Phys. Chem.* **1996**, *100*, 15562.

host−guest complex between the amino acid and the receptor **3**. It should be noted that the study of the methylammonium perchlorate complexation with receptor **3** showed a negligible interaction. Further studies in our research group are now being undertaken to study the amino acid recognition by the other members of this novel crown ether generation and to use these compounds as suitable ionophores for the preparation of a polymeric membrane sensor for the selective potentiometric determination of specific amino acids.

Conclusion

Novel crown ethers containing heteroaromatic cations have been prepared and characterized. The first case, the pyrilium benzo-9-crown-3 derivative, **3**, was prepared in 29.4% yield from the condensation of 2 mol of acetophenone and 1 mol of 4′-HCO-B9C3 in the presence of $POCl_3$. The second, the thiopyrilium B9C3 derivative, **5**, was synthesized from the substitution reaction on **3** by Na_2S. The pyridinium B9C3 derivative, **6**, was obtained from the substitution reaction on **3** by NH_4NO_3, 80% yield, followed by protonation. The ESMS was found to be a good MS technique in the characterization of these compounds. The UV−vis absorption data of **3** and **5** are close to each other while totally different from **4**. The B9C3 unit in the compounds **3** and **5** have close behavior in the solution- and solid-phase NMR which resembles 4′-HCO-B9C3, **2**. The heteroaromatic cations at the 4′-position of B9C3 in the cases of **3** and **5**, in fact, behave much like a formyl substitution. The NMR data of these three crown ethers are quite different from that of **4**. The X-ray crystal structure of **3** and **5** showed small deviation from planarity for the four aromatic rings while the three aromatic rings connected to pyridine ring in **4** are out of the pyridine ring. The planarity degree order of the two phenyl rings connected to the heteroaromatic ring at the 2- and 6-positions is as **3** > **5** > **4**. The solid-phase stereochemistry of B9C3 cavity in **3** and **5** are almost the same and different from that in **4**. The behavior of each of the two units in this generation was found to be affected by each other. Spectrophotometric studies in methanol solution revealed that lysine, among several amino acids including histidine, serine, argenine, cystein, glycine, and leucine can selectively bind to the receptor molecule **3**.

Experimental Section

Instrumentation. Solution NMR spectra were recorded on a 400-MHz Bruker spectrometer. Samples for both ^1H and ^{13}C NMR were obtained in 5-mm tubes at a concentration of 0.1 M in $CDCl_3$ or DMSO-d_6 solution. All chemical shifts are reported in ppm downfield from TMS. The mass spectra were recorded on a MS80RFA mass spectrometer by EI at 70 eV and positive ion ES method using CH_3OH, HCOOH, CH_3OH + KCl, and CH_3OH + NaCl as carriers. The IR spectra were obtained with a FTIR Shimadzu spectrometer using KBr disks. The melting points were measured on a digital Electrothermal 9100 apparatus and are uncorrected. Elemental analyses were performed at University of Ottawa. The solid-phase ^{13}C NMR spectra were obtained at 50.3 MHz using a Bruker ASX-200 under the conditions described previously.[37] The spinning rate was 5 kHz. Chemical shifts were measured relative to external hexamethylbenzene, HMB methyl resonance at 16.9 ppm, and then converted to the TMS scale. The dipolar dephasing experiment was carried out by interruption of the ^1H decoupling for 40 μs immediately following the cross-polarization sequence.

X-ray Structure Determinations. Suitable crystals were selected, mounted on thin glass fibers using viscous oil, and cooled to the data collection temperature of 203(2) K. Data were collected on Bruker AX SMART 1k CCD diffractometer using 0.3° scans at 0.90° and 180° in. Unit cell parameters were determined from 60 data frames collected at different sections of the Edwald sphere. Semiempirical absorption corrections based on equivalent reflections were applied.[38] Unit cell parameters and systematic absences in the diffraction data are consistent with the space groups. All structures were solved by direct methods, completed with difference Fourier syntheses and refined by full-matrix least squares procedures based on F^2. All non-hydrogen atoms were refined with anisotropic displacement parameters, and hydrogen atoms were treated as idealized contributions. All scattering factors and anomalous dispersion factors are contained in the SHEXTL 5.1 program library. A summary of crystals' data and data collection parameters is given in Table 2.

Fluorescence Spectra. All fluorescence spectra were recorded on a Perkin-Elmer luminescence spectrometer LS-30, equipped with a Xenon lamp, at a fixed spectral band-pass of 10 nm for both monochromators.

Materials. B9C3 was prepared according to the previously reported procedure.[4] Other reagents were purchased from Merck.

Syntheses. 4′-Formyl-B9C3 (2). A 250-mL flask was charged with B9C3 (13.5 g, 75 mmol), hexamethylenetetramine (11 g, 75 mmol), and 56 mL of trifluoroacetic acid under nitrogen and heated for 12 h at 90 °C. The reaction mixture was cooled to room temperature and was extracted with dichloromethane (3 × 100 mL). The combined organic extracts were washed with water (4 × 300 mL) and dried over anhydrous Na_2SO_4, and the solvent was removed by a rotary evaporator. The resulting viscous oil was then extracted with boiling hexane (4 × 100 mL); 11 g (75% yield) of white crystalline product **2** was obtained upon cooling the combined hexane extracts, mp 46−47 °C: ^1H NMR ($CDCl_3$) δ 4.0 (m, 4H, CH_2OCH_2), 4.3 (m, 2H, C-O-CH_2), 4.6 (m, 2H, C-O-CH_2), 7.1 (d, 1H, CH, ^3J = 8.2 Hz), 7.53 (d, 1H, ^4J = 2.1 Hz), 7.57 (dd, 2H, CH, ^3J = 8.2, ^4J = 2.1 Hz); ^{13}C NMR (DMSO-d_6) δ 156.4, 151.0, 131.5, 125.7, 122.1, 74.5, 73.7, 71.4, 71.0 ppm.

2,6-Diphenyl-4-B9C3-pyrilium Perchlorate (3). Crown ether **2** (2.47 g, 12 mmol) was added to acetophenone (4.6 g, 30 mmol) in a 50-mL flask. The reaction mixture was warmed in a water bath (56 °C) with stirring, and 2 mL of $POCl_3$ was added dropwise. The stirring was continued for 3 h followed by evaporation of excess $POCl_3$ by a rotary evaporator. The brown-reddish oily residue was dissolved in 120 mL of hot absolute ethanol and was heated to boiling. To the hot ethanol solution was then added 2 mL of 60% perchloric acid, and the mixture was allowed to cool to room temperature. The crystalline product was filtered, washed with diethyl ether, and finally vacuum-dried. The orange product was recrystalized from CH_2Cl_2/Et_2O. After suction filtration and washing the orange crystals with diethyl ether, 1.75 g (29.4%) of **3**, mp 248−50 °C, was obtained: ^1H NMR ($CF_3COOH/CDCl_3$) δ 4.3 (m, 4H, CH_2), 4.6 (m, 2H, CH_2O), 4.9 (m, 2H, CH_2O), 7.40 (d, 1H, ^4J = 8.7 Hz), 7.78−7.87 (m, 6H, Ph), 8.00 (dd, 1H, ^3J = 8.7, ^4J = 2.1 Hz), 8.09 (d, 1H, ^3J = 2.1 Hz), 8.36 (d, 4H, ^3J = 7.5), 8.54 (s, 1H, pyrilium); ^{13}C NMR ($CF_3COOH/CDCl_3$) δ 72.1, 72.4, 73.0, 75.4, 113.8, 124.8, 126.2, 127.3, 128.0, 128.5, 129.0, 130.8, 136.4, 151.8, 158.8, 165.3, 171.7; IR (KBr disk) 3061(w), 2975(m), 1718(w, broad), 1629(s), 1595(s), 1562(m), 1515(w), 1492(s), 1411(m), 1319(m), 1247(s), 1191(w), 1153(w), 1126(m), 1095(s), 1051(m), 997(w), 952(w), 871(w), 817(w), 686(m), 622(m), 572(w) and 497(w) cm^{-1}; EI-MS *m*/*z* (%) 410(1.5), 252(80), 167(53), 152(12), 109(100), 91(27), 45(26); ESI-MS (CH_3OH as carrier) *m*/*z* (%) 414.0(1), 413.0(6), 412.0(37), 411.0-(2,6-diphenyl-4-B9C3 pyrilium cation)(100), 263.0(3), 84.8(4),

(37) Buchanan, G. W.; Gerzain, M.; Facey, G. A.; Bensimon, C. *J. Mol. Struct.* **1998**, *471*, 95.

(38) Blessing, R. *Acta Crystallogr., Sect. A* **1995**, *A51*, 33.

73.8(8), 58.8(8). Anal. Calcd for $C_{27}H_{23}O_8Cl$: C, 63.47; H, 4.54. Found: C, 63.34; H, 4.63.

2,6-Diphenyl-4-B9C3-pyridine (4). A mixture of pyrilium perchlorate derivative **2** (1.8 g, 3.6 mmol), ammonium acetate (2.8 g, 3.6 mmol), and 8 mL of glacial acetic acid was placed in a 25-mL flask and refluxed for 3 h in an oil bath. The reaction mixture was then cooled to room temperature followed by the addition of 30 g of ice−water mixture. The product formed was subsequently filtered by suction. The crude product was dissolved in absolute ethanol, boiled with carbon active, and filtered, and the filtrate was put aside. The colorless cubic crystalline product was formed after 24 h. Suction filtration was applied to obtain 1.28 g (80% yield) pyridine derivative **4**, mp 146−8 °C: ^{1}H NMR ($CDCl_3$) δ 3.99 (m, 4H, CH_2), 4.49 (m, 4H, CH_2O), 7.18 (d, 1H, ^3J = 8.3 Hz), 7.41 (dd, 1H, ^3J = 8.3, ^4J = 2.3 Hz), 7.47(d, 1H, ^4J = 2.3 Hz), 7.50−7.61(m, 6H, Ph), 7.89(s, 2H, pyridine), 8.26(dd, 4H, ^3J = 5.4, ^4J = 1.6 Hz, Ph); ^{13}C NMR ($CDCl_3$) δ 72.1, 72.2, 73.7, 74.1, 116.5, 121.6, 122.5, 123.3, 127.0, 128.5, 128.9, 134.4, 139.5, 149.0, 151.0, 157.3; IR (KBr disk) 3020, 2927(m), 2357(w), 1655(w, broad), 1595(m), 1543(m), 1498(s), 1450(w), 1377(m), 1280(s), 1178(m), 1134(m), 1085(w), 1039(w), 1014(m), 875(m), 825(m), 771(m), 735(m), 688(s), 601(w), 534(w), 464(w) cm^{-1}; EI-MS *m*/*z* (%) 409(M+, 96), 365(100), 350(15), 309(20), 280(25), 202(7), 189(6), 77(7), 45(8); ESI-MS (HCOOH as carrier) *m*/*z* (%) 412.2(2), 411.2(12), 410.2(M + 1, 43), 87.9(5), 73.9(3), 56.0(100), 42.1(92); ES-MS (MeOH + KCl as carrier) *m*/*z* (%) 857.1(2M + K$^+$, 60), 450.0(12), 449.0(30), 448.0(M + K$^+$, 100), 410.1(M + 1, 95), 104.1(28), 81.1(70). Anal. Calcd for $C_{27}H_{23}NO_3$: C, 79.20; H, 5.66; N, 3.42. Found: C, 79.15; H, 5.53; N, 3.50.

2,6-Diphenyl-4-B9C3-thiopyrilium Perchlorate (5). The compound **3** (2.5 g, 5 mmol) was dissolved in 100 mL of acetone in a 250-mL beaker. A 10% sodium sulfide solution, in distilled water, was dropwise added to the **3** solution until no Na_2S precipitate was observed at the bottom of beaker. The reaction mixture was stirred for 20 min followed by the dropwise addition of 20% perchloric acid. The solution color turned to purple while perchloric acid solution was being added. Subsequently, 100 mL of distilled water was added to the purple solution. The crystalline product was precipitated upon standing the solution for a while. The crude product was collected by filtration (sample I). Since sample I showed starting pyrilium material as impurity, it was dissolved in acetone and retreated with Na_2S as explained before, and this procedure repeated once more. Finally, the crystalline product was recrystalized from a mixture of CH_2Cl_2/Et_2O to obtain 0.37 g of **5** in 14% yield, mp 233−37 °C (sample II). Anal. Calcd for $C_{27}H_{33}O_7SCl$ (sample II): C, 61.54; H, 4.40. Found: C, 61.55; H, 4.45. ESMS (sample I in MeOH as carrier): *m*/*z* 100.04 (13), 116.03 (48), 155.01 (8), 180.96 (5), 216.95 (4), 411.04 (2,6-diphenyl-4-B9C3-pyrilium cation as impurity, 50), 426.99 (2,6-diphenyl-4-B9C3-thiopyrilium cation, 100), 428.03 (42), 429.03 (15), 430.03 (3), 464.96 (4). ESI-MS (sample II in MeOH as carrier): *m*/*e* 42.0 (4), 411.0 (5), 426.9 (100), 427.9 (30), 428.9 (9), 429.9 (2); ^{1}H NMR (DMSO-d_6) δ 3.90 (m, 4H, CH_2O), 4.40 (m, 2H, CH_2O), 4.80 (m, 2H, CH_2O), 7.21 (d, 1H, ^3J = 8.7 Hz), 7.74−7.85 (m, 6H, Ph), 8.17 (dd, 1H, ^3J = 8.7, ^4J = 2.3 Hz), 8.27 (m, 4H), 8.56 (d, 1H, ^3J = 2.3 Hz), 9.18 (s, 2H); ^{13}C NMR (DMSO-d_6) δ 70.84, 70.94, 72.26, 74.97, 122.46, 126.53, 127.07, 128.91, 129.51, 130.08, 133.40, 134.22, 151.56, 156.26, 159.26, 166.74.

Acknowledgment. A.M., M.F.R., and M.G. wish to gratefully acknowledge the support of this work by the research council of the University of Tehran. A.M. and M.F.R. also thank Prof. G. W. Buchanan at Carleton University, Ottawa, Canada for the solid-phase NMR and elemental analysis.

Supporting Information Available: ESI-MS spectrum of **3**; UV−vis spectra; ^{1}H and ^{13}C NMR data of **3**−**5** in DMSO-d_6; 2D ^{1}H−^{1}H COSY spectrum; and linear plots of the six series of repeated experiments for the calculation of the average K_s obtained for the lysine-**3** complexation. This material is available free of charge via the Internet at http://pubs.acs.org.

JO010869F